European Journal of Radiology Open 8 (2021) 100325

Contents lists available at ScienceDirect

European Journal of Radiology Open

journal homepage: www.elsevier.com/locate/ejro

Etiological profile and main imaging findings in patients with granulomatous diseases who underwent lung biopsy

Camila Vilela de Oliveira [a,*], Natally Horvat [a,b], Leonardo de Abreu Testagrossa [c], Davi dos Santos Romão [a], Marina Bastos Rassi [a], Hye Ju Lee [a,d]

[a] Department of Radiology, Hospital Sírio-Libanês, São Paulo, SP, Brazil
[b] Department of Radiology, Memorial Sloan Kettering Cancer Center, New York, NY, USA
[c] Department of Pathology, Hospital Sírio-Libanês, São Paulo, SP, Brazil
[d] Department of Radiology, Universidade de São Paulo, São Paulo, SP, Brazil

ARTICLE INFO

Keywords:
Granuloma
lung biopsy
solitary pulmonary nodule
histoplasmosis
pulmonary tuberculosis

ABSTRACT

Background: Granulomatous Lung Diseases (GLD) encompasses a wide range of infectious and non-infectious conditions characterized by chronic inflammatory response. However, different GLD may share similar imaging findings. In this context, the purpose of this study was to outline the etiological profile and their imaging features in patients with GLD who underwent lung biopsy.

Methods: Patients with granulomatous lesions in lung biopsies and previous chest CT performed from 2014 to 2017 at our institution had imaging data reviewed by three blinded radiologists. The imaging features were analyzed according to the Fleischner Society glossary. Categorical data were represented by absolute (n) and relative (%) frequency. The contingency matrices were analyzed by Pearson's Chi-square test. Interreader agreement was assessed by calculating the intraclass correlation coefficient, using kappa (κ) statistic.

Results: Thirty-eight of 75 (50.7%) patients were women with a mean age of 59 ± 39 years. Infection was the most common cause of GLD (47/75, 62.7%) and *Histoplasma capsulatum* (27/75, 36%) was the most prevalent etiology. Nodular pattern was the most common imaging feature in histoplasmosis cases (25/27, 92.6%), whereas it occurred in half of cases (24/48) of GLD of other causes ($p < 0.05$). Among patients with tuberculosis, the second etiology of GLD in our study population, the most common imaging pattern was centrilobular micronodules (3/7, 42.9%), significantly more frequent than in other causes of GLD (6/68, 8.8%). Interreader agreement in detecting imaging features was almost perfect (κ = 0.88-1.00), except the nodular pattern, which had substantial agreement (κ = 0.73).

Conclusions: In our study population, the main etiologies found in patients with granulomatous disease who underwent lung biopsy were fungal or mycobacterial disease, specially histoplasmosis and tuberculosis, and nodular pattern with focal distribution was the most common imaging finding which was detected with substantial interreader agreement.

1. Introduction

Granulomatous Lung Diseases (GLD) encompasses a wide range of infectious and non-infectious conditions characterized by chronic inflammatory response [1]. Generally, the etiology is defined combining clinical symptoms, laboratorial findings, and imaging features. Patients undergo lung biopsy when the manifestation is atypical or when excluding lung cancer is needed [2].

Mycobacterial and fungal infections are the most common infectious causes of GLD, including tuberculosis (TB), nontuberculous mycobacteriosis, histoplasmosis, cryptococcosis, coccidioidomycosis, blastomycosis, and aspergillosis [3]. TB is a public health problem worldwide, mainly in underdeveloped countries, and was responsible for 1.5 million deaths in 2018 [4–6]. With the development of the HIV epidemic, these

Abbreviations: CT, Computed Tomography; FOV, Field of View; GLD, Granulomatous lung diseases; GLUS, Granulomatous Lesions of Unknown Significance; JR, Junior Radiologists; κ, Kappa; TB, Tuberculosis.

* Corresponding author at: Department of Radiology, Hospital Sírio-Libanês, Rua Dona Adma Jafet, 91, Bela Vista, 01308-050, São Paulo, SP, Brazil.
E-mail address: camilavilela08@gmail.com (C.V. de Oliveira).

https://doi.org/10.1016/j.ejro.2021.100325
Received 6 December 2020; Received in revised form 8 January 2021; Accepted 11 January 2021

infections increased in incidence and lethality. Non-infectious GLD might be the result of several different physiopathological conditions [7–9] and are summarized in Table 1.

Finally, there are granulomatous lesions of uncertain etiology, comprising a group known as Granulomatous Lesions of Unknown Significance (GLUS). This term was used for the first time in 1990 to designate biopsies results which contained epithelioid granulomas without a definitive cause, even after subsequent investigation [10].

Computed tomography (CT) is the most common imaging modality used to evaluate GLD. However, different GLD may share similar imaging findings. In this context, the purpose of this study was to outline the etiological profile and their imaging findings in patients with granulomatous diseases who underwent lung biopsy. This information can guide further clinical investigation in atypical granulomatous lung cases to possibly avoid invasive procedures.

2. Material and Methods

2.1. Study population

The institutional and national review boards approved our retrospective study and waived the requirement for informed consent. We searched our hospital database for consecutive lung biopsies performed between January 2014 and December 2017 at our institution. The following types of lung biopsies were included: intraoperative biopsy, bronchoscopy with transbronchial biopsy and percutaneous CT-guided needle biopsy. The inclusion criterion was the existence of granulomatous lesions in the pathology report (88 of 994 patients). Patients without chest CT previous to lung biopsy were excluded and the final study population was 75 patients. The patient accrual is summarized in Fig. 1.

2.2. Demographic and Pathologic Data

Pathological reports of all patients who underwent lung biopsy between January 2014 and December 2017 were obtained from the hospital database. A keyword search was performed and reports containing “granuloma(s)” and/or “granulomatous” were selected. The following data were assessed: gender, age and the etiology of the GLD.

All cases were analyzed by two pathologists with subspecialty training in pulmonary pathology and with at least 8 years of training. Each pathological specimen with diagnosis of GLD underwent specific tests for infection, besides the usual Hematoxylin-Eosin stain.

Table 1
Main differential diagnosis of granulomatous lung diseases.

Infectious	Non-Infectious
Fungal	
Histoplasmosis	
Paracoccidioidomycosis	
Coccidioidomycosis	Sarcoidosis
Aspergillosis	Bronchocentric Granulomatosis
Cryptococcosis	Inflammatory Bowel Disease
Blastomycosis	Hypersensitivity Pneumonitis
Pneumocystosis	Chronic Beryllium disease
Actinomycosis	Silicosis
Mycobacterial	Foreign body reaction
Tuberculosis	Granulomatosis with Polyangiitis
Nontuberculous mycobacteriosis	Eosinophilic Granulomatosis with Polyangiitis
Hansen’s Disease	Wegener Granulomatosis
Parasitic	Churg-Strauss Syndrome
Paragonimiasis	Lymphoid Interstitial Pneumonia
Bacterial	Cancer associated with GI
Syphilis	Rheumatoid Nodule
Tularaemia	Pulmonary Langerhans Cell Histiocytosis
Cat-scratch Disease	
Whipple’s Disease	
Aspiration Pneumonia	

GI = Granulomatous Inflammation

2.3. Computed Tomography Exams

CT scans were performed on one of the following devices: a dual-source 256 row detector CT system (SOMATOM® Definition Flash; Siemens Healthcare, Erlangen, Germany) or a 128-row detector CT system (SOMATOM® Definition AS; Siemens Healthcare, Erlangen, Germany). The acquisition parameters were the same for both devices as follows: 115–160 mAs; 120 kVp; tube rotation time, 0.5 s; pitch, 1.2; and field of view (FOV), 400–430 mm. When contrast was required, the timing was determined with a test bolus that consisted of 10–15 ml of iohexol solution (OmnipaqueTM 300; GE Healthcare, Milwaukee, WI) with an iodine concentration of 300 mg ml^{-1} injected at a flow rate of 4.0–5.5 ml/s^{-1}. Contrast imaging was performed with 1.0 - 1.5 ml/kg injected at the same flow rate. Images were reconstructed in the axial view using a slice thickness of 1 mm and an increment of 0.7 mm.

2.4. Image review

Two junior thoracic radiologists with 1 year experience in chest radiology, blinded to the pathological data, reviewed the radiological exams. The imaging features were analyzed according to the Fleischner Society glossary [11]. A senior thoracic radiologist with 10 years of experience reviewed all cases of disagreement to reach a consensus.

The CT findings were categorized according the main radiological pattern: consolidation, ground-glass opacity, mass, nodular or micronodular. Micronodular pattern was subcategorized into random, perilymphatic or centrilobular. The location of the imaging findings was divided into right, left or bilateral; the distribution was focal, multifocal or diffuse; and the associated findings were cavity, mediastinal/hilar lymphadenopathy, and pleural effusion.

Consolidation was defined as a homogeneous increase in pulmonary parenchymal attenuation that obscured the margins of the vessels and airway walls. Ground-glass opacity was noted as a hazy increased opacity of lung, with preservation of the bronchial and vascular margins. Nodule corresponded to a rounded or irregular opacity, measuring up to 3 cm in diameter, while mass corresponded to a solid or partly solid lesion greater than 3 cm. Micronodular pattern was defined by the presence of innumerable small rounded opacities that ranged from 2 to 10 mm [11].

Cavity was a gas-filled space within pulmonary consolidation, mass or nodule. Lymphadenopathy consisted of mediastinal lymph nodes greater than 1 cm in short-axis diameter and hilar nodes bigger than 3 mm. Pleural effusion was noted when there were free liquid in the pleural space [11].

Figs. 2 and 3 demonstrate the main radiological findings evaluated in our study.

2.5. Statistical Analysis

Categorical data were represented by absolute (n) and relative (%) frequency. Two-tailed p-values ≤ 0.05 were considered significant. The contingency matrices were analyzed by Pearson’s Chi-square test. Interreader agreement was assessed by calculating the intraclass correlation coefficient. On categorical features, it was assessed using kappa (κ) statistic or weight kappa statistic with squared weights (for more than two levels) between the two junior radiologists (JR). Kappa (κ) values were interpreted as follows: 0.00-0.20, slight agreement; 0.21-0.40, fair agreement; 0.41-0.60, moderate agreement; 0.61-0.80, substantial agreement; and 0.81-1.00, almost perfect agreement [12]. Statistical analyses were done using SPSS for Windows version 19.0 (Chicago, IL, USA).

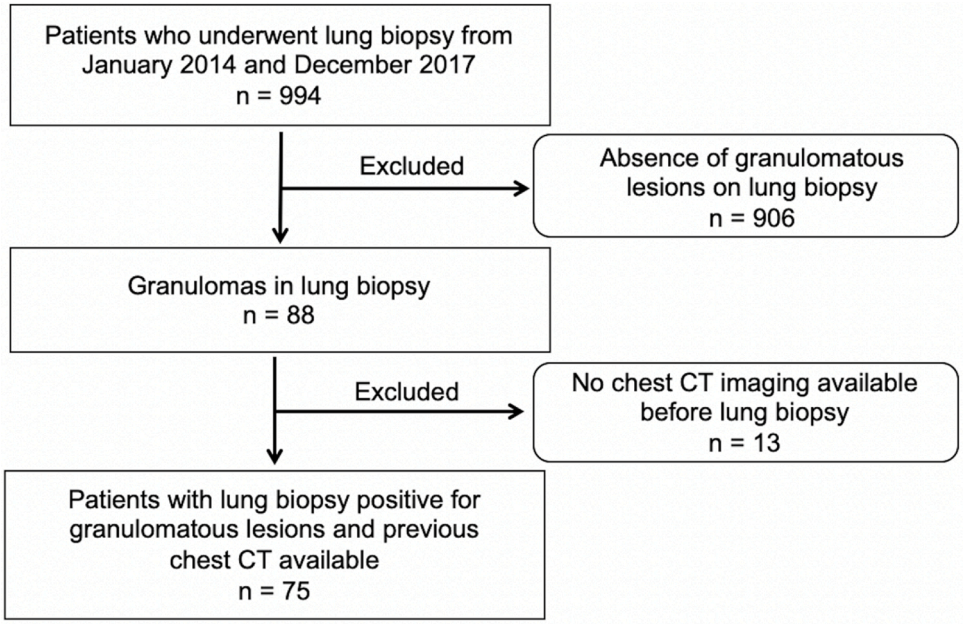

Fig. 1. Flowchart of patient selection.

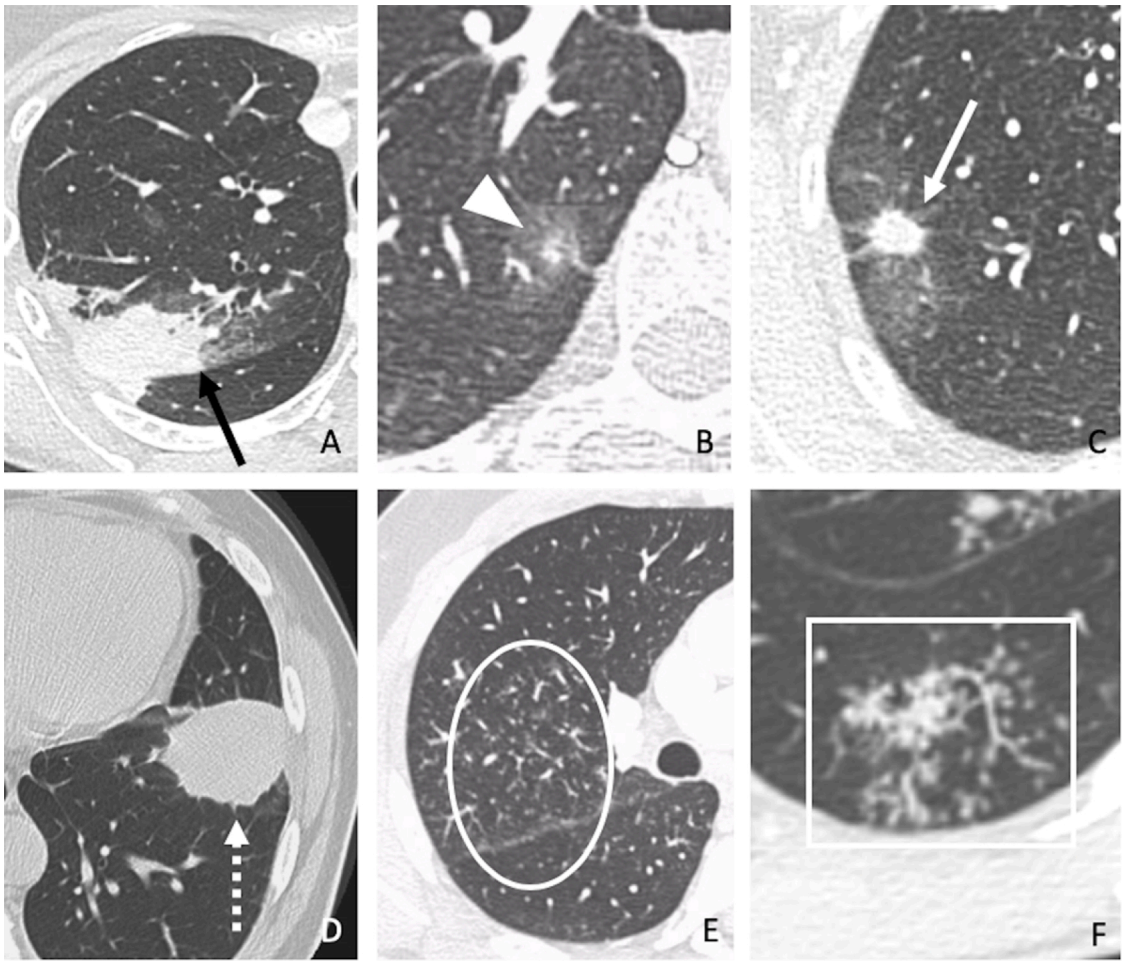

Fig. 2. Main radiological findings assessed in our study. (A) Consolidation (black arrow) in a 54-year-old patient with sarcoidosis. (B) Ground-glass opacity (arrowhead) in a 61-year-old patient with paracoccidioidomycosis. (C) Nodule (white arrow) in a 77-year-old patient with histoplasmosis. (D) Mass (dashed arrow) in a 51-year-old patient with cryptococcosis. (E) Perilymphatic micronodules in a 41-year-old patient with granulomatous lesions of unknown significance (GLUS) (circle). (F) Centrilobular micronodules (rectangle) in a 30-year-old patient with tuberculosis.

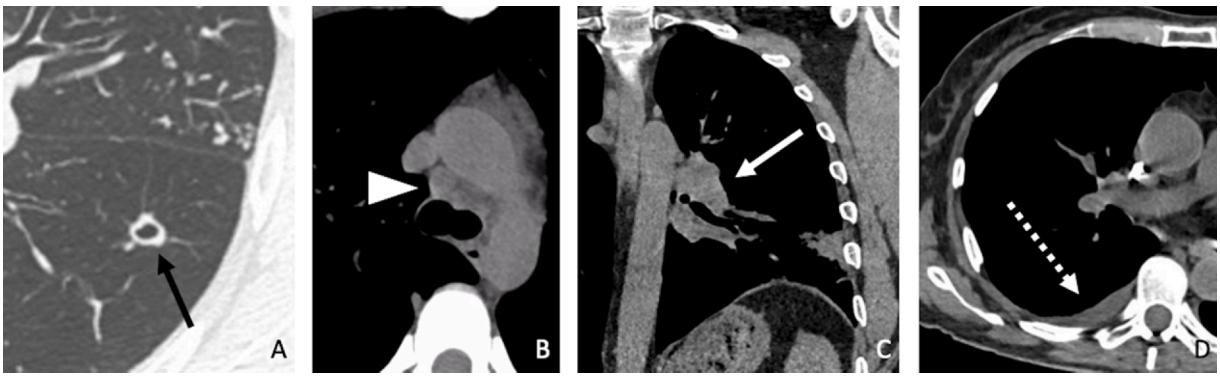

Fig. 3. Main associated radiological findings evaluated in our study. (A) Cavitated nodule (black arrow) in a 34-year-old patient with tuberculosis. (B) Mediastinal lymphadenopathy (arrowhead) in a 39-year-old patient with sarcoidosis. (C) Hilar lymphadenopathy (white arrow) in a 75-year-old patient with histoplasmosis. (D) Pleural effusion (dashed arrow) in a 76-year-old patient with unclassified mycobacteriosis.

3. Results

3.1. Population Data

The study population consisted of 75 patients, 49,3% men (37/75) and 50,7% women (38/75). The mean age was 57 (range 18-96). The majority of the samples were obtained by CT-guided biopsy (47/75, 62.7%), 23/75 (30.7%) by intra-operative biopsy and 5/75 (6.7%) were acquired by bronchoscopy.

Infection was the most common cause of GLD (47/75, 62.7%) and GLUS corresponded to 24% (18/75) of the cases. Among infectious causes of GLD, the great majority was fungal or mycobacterial, caused by *Histoplasma capsulatum* (27/75, 36%) and *Mycobacterium tuberculosis* (7/75, 9.3%). Unclassified mycobacterial infection represented 6.7% of cases (5/75). Other fungal infections included Paracoccidioidomycosis (3/75, 4.0%), Aspergillosis (3/75, 4.0%) and Cryptococosis (1/75, 1.3%). Only one case of parasitic infection occurred, represented by Paragominiasis.

Among non-infectious causes, sarcoidosis occurred in 4 cases (5.4%) and granulomatous inflammation associated with cancer occurred in 6 cases (8.0%). Other non-infectious causes did not occur in our study population. Table 2 summarizes the etiological profile of the included patients.

3.2. Chest CT findings

The main radiological pattern, location and distribution, as well as associated imaging findings are summarized in Table 2.

Overall, nodular pattern was the most common CT finding (49/75, 65.3%), followed by centrilobular micronodules (9/75, 12%), as seen in Fig. 4. The majority of cases had unilateral pulmonary findings (59/75, 78.7%), slightly more common in the left lung (31/59, 52.5%). Focal distribution was the most frequent (50/75, 66.7%).

Among associated findings, hilar or mediastinal lymphadenopathy occurred respectively in 16% (12/75) and 10.7% (8/75) of the cases; pleural effusion (8/75) and cavitation (8/75) occurred in 10.7% of cases.

Nodular pattern was the most common imaging feature in histoplasmosis cases (25/27, 92.6%), whereas it occurred in half of cases (24/48) of GLD of other causes ($p < 0.05$). Regarding distribution of the lung lesions, 26/27 (96.3%), were focal in histoplasmosis, while in other causes of GLD focal distribution occurred in 50% (24/48) of cases ($p < 0.05$) (Table 3).

Among patients with tuberculosis, the second etiology of GLD in our study population, the most common imaging pattern was centrilobular micronodules (3/7, 42.9%), significantly more frequent than in other causes of GLD (6/68, 8.8%). Cavitation also was highly suggestive of mycobacterial infection, occurring in 57.1% (4/7) of cases of tuberculosis, compared to only 2 cases (2.9%) of all other causes of GLD, considering that one of these 2 cases occurred in a patient with unclassified mycobacteriosis.

All 4 cases of sarcoidosis had multifocal distribution and patterns varied between consolidation, nodular and perilymphatic micronodules. Mediastinal or hilar lymphadenopathy weren't detected in just one case.

Among the 3 cases of aspergillosis, each one presented with a different main radiological pattern, which were consolidation, mass and centrilobular micronodules. The majority of paracoccidioidomycosis cases exhibited nodular pattern (2/3, 66.7%).

Fig. 5 demonstrates radiologic-pathologic correlation of three sample cases of our population.

3.3. Interreader agreement

Interreader agreement in detecting the associated findings and radiological patterns was almost perfect ($\kappa = 0.88$-1.00), except the nodular pattern, which had substantial agreement ($\kappa = 0.73$) (Supplementary table).

4. Discussion

In most studies, non-infectious GLD are the most prevalent among patients submitted to lung biopsy [1,13]. This difference is probably due to the high prevalence of fungal diseases, such as histoplasmosis and tuberculosis in our population. The etiological profile found in our study was similar to that presented by Nazarullah et al. [14], where infectious GLD were more prevalent than non-infectious.

Among the patients with biopsy proven granulomatous disease, as in the studies of Sakakibara et al. [15] and Zhu et al. [1], the most commonly found radiological pattern was solitary pulmonary nodule, which can be explained by the crescent indication of lung biopsies for investigation of indeterminate solitary pulmonary nodules suspected for malignancy [16]. This pattern was significantly associated with histoplasmosis ($p < 0.05$). Centrilobular micronodules and cavity were also frequent and significantly associated with tuberculosis ($p < 0.05$). Sarcoidosis and other infectious causes (such as aspergillosis, paracoccidiodomycosis, cryptococcosis and paragonimiasis) did not present statistically significant association with a specific radiological pattern.

The clinical relevance of our results relies on the approach of the differential diagnosis in cases of patients with solitary pulmonary nodules in countries with high prevalence of GLD. Histoplasmosis should be considered a possible differential diagnosis in cases of solitary pulmonary nodule in patients with low risk for lung cancer [17]. Besides, the recognition of radiological patterns strongly associated with granulomatous diseases can be useful for clinicians to guide further investigations.

Being a single-center retrospective study, it is subjected to selection

Table 2
Imaging features of granulomatous lung diseases.

	Histoplasmosis		Tuberculosis		Cancer + GI		Unclassified Mycobacteriosis		Sarcoidosis		Aspergillosis		Paracoccidioidomycosis		Cryptococcosis		Paragonimiasis		GLUS		Total	
Radiological Pattern	**n**	**%**	**n**	**%**	**n**	**%**	**n**	**%**	**n**	**%**	**n**	**%**	**n**	**%**	**n**	**%**	**n**	**%**	**n**	**%**	**n**	**%**
Consolidation	1	(3.7)	2	(28.6)	0		1	(20.0)	2	(50.0)	1	(33.3)	0		0		0		0		7	(9.3)
Ground-glass opacity	0		0		1	(16.7)	0		0		0		1	(33.3)	0		0		0		2	(2.7)
Nodule	25	(92.6)	2	(28.6)	3	(50.0)	1	(20.0)	1	(25.0)	0		2	(66.7)	0		0		15	(83.3)	49	(65.3)
Mass	1	(3.7)	0		2	(33.3)	1	(20.0)	0		1	(33.3)	0		1	(100.0)	0		0		6	(8.0)
Random micronodules	0		0		0		0		0		0		0		0		0		0		0	
Perilymphatic micronodules	0		0		0		0		1	(25.0)	0		0		0		0		1	(5.6)	2	(2.7)
Centrilobular micronodules	0		3	(42.9)	0		2	(40.0)	0		1	(33.3)	0		0		1	(100.0)	2	(11.1)	9	(12.0)
Associated Findings																						
Cavity	0		4	(57.1)	1	(16.7)	1	(20.0)	0		0		0		0		0		0		6	(8.0)
Mediastinal lymphadenopathy	3	(11.1)	1	(14.3)	1	(16.7)	0		1	(25.0)	1	(33.3)	0		0		0		1	(5.5)	8	(10.7)
Hilar lymphadenopathy	5	(18.5)	0		1	(16.7)	1	(20.0)	2	(50.0)	1	(33.3)	0		0		0		2	(11.1)	12	(16.0)
Pleural effusion	2	(7.4)	1	(14.3)	0		2	(40.0)	0		2	(66.7)	0		0		0		1	(5.6)	8	(10.7)
Location and Distribution																						
Unilateral (Right)	11	(40.7)	2	(28.6)	3	(50.0)	2	(40.0)	1	(25.0)	1	(33.3)	2	(66.7)	0		0		6	(33.3)	28	(37.3)
Unilateral (Left)	16	(59.3)	2	(28.6)	2	(33.3)	1	(20.0)	0		1	(33.3)	1	(33.3)	1	(100.0)	0		7	(38.9)	31	(41.3)
Bilateral	0		3	(42.9)	1	(16.7)	2	(40.0)	3	(75.0)	1	(33.3)	0		0		1	(100.0)	5	(27.8)	16	(21.3)
Focal	26	(96.3)	3	(42.9)	5	(83.3)	2	(40.0)	0		2	(66.7)	3	(100.0)	0		0		9	(50.0)	50	(66.7)
Multifocal	1	(3.7)	3	(42.9)	1	(16.7)	1	(20.0)	4	(100.0)	0		0		1	(100.0)	1	(100.0)	8	(44.4)	20	(26.7)
Diffuse	0		1	(14.3)	0		2	(40.0)	0		1	(33.3)	0		0		0		1	(5.6)	5	(6.7)
Right upper lobe	5	(18.5)	4	(57.1)	3	(50.0)	3	(60.0)	3	(75.0)	1	(33.3)	1	(33.3)	0		1	(100.0)	6	(33.3)	27	(36.0)
Right middle lobe	4	(14.8)	4	(57.1)	0		2	(40.0)	4	(100.0)	1	(33.3)	0		0		1	(100.0)	5	(27.8)	21	(28.0)
Right lower lobe	5	(18.5)	3	(42.9)	2	(33.3)	3	(60.0)	3	(75.0)	2	(66.7)	1	(33.3)	0		1	(100.0)	6	(33.3)	26	(34.7)
Left upper lobe	6	(22.2)	5	(71.4)	2	(33.3)	3	(60.0)	3	(75.0)	1	(33.3)	0		1	(100.0)	1	(100.0)	5	(27.8)	27	(36.0)
Left lower lobe	10	(37.0)	2	(28.6)	1	(16.7)	3	(60.0)	2	(50.0)	2	(66.7)	1	(33.3)	1	(100.0)	1	(100.0)	10	(55.6)	33	(44.0)
Total	**27**	**(36.0)**	**7**	**(9.3)**	**6**	**(8.0)**	**5**	**(6.7)**	**4**	**(5.3)**	**3**	**(4.0)**	**3**	**(4.0)**	**1**	**(1.3)**	**1**	**(1.3)**	**18**	**(24.0)**	**75**	**(100.0)**

GI: Granulomatous Inflammation; GLUS: Granulomatous Lesions of Unknown Significance.

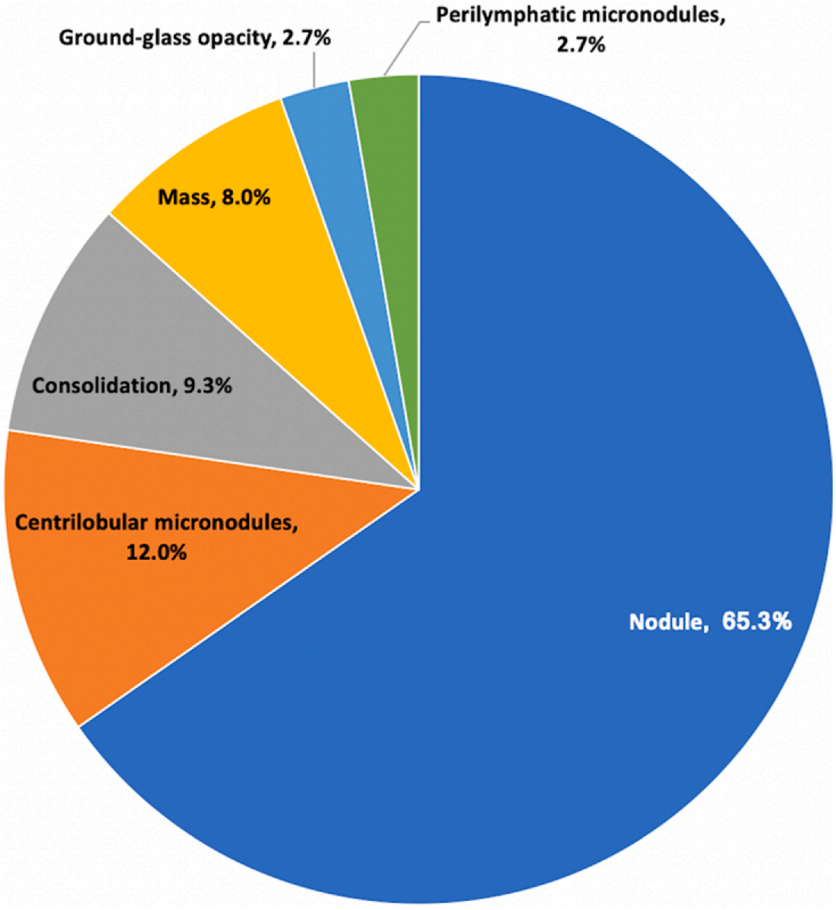

Fig. 4. Distribution of the radiological patterns in our study population.

Table 3
Comparison of imaging features on chest computed tomography of patients with pulmonary histoplasmosis and tuberculosis.

	Histoplasmosis		Other etiologies		P-value	Tuberculosis		Other etiologies		P-value
Radiological Pattern	**n**	**%**	**n**	**%**	**p**	**n**	**%**	**n**	**%**	**p**
Consolidation	1	(3.7)	6	(12.5)	0.208	2	(28.6)	5	(7.4)	0.066
Ground-glass opacity	0		2	(4.2)	0.282	0		2	(2.9)	0.646
Nodule	25	(92.6)	24	(50.0)	**< 0.001**	2	(28.6)	47	(69.1)	**0.032**
Mass	1	(3.7)	5	(10.4)	0.304	0		6	(8.8)	0.413
Random micronodules	0		0			0		0		
Perilymphatic micronodules	0		2	(4.2)	0.282	0		2	(2.9)	0.646
Centrilobular micronodules	0		9	(18.8)	**0.016**	3	(42.9)	6	(8.8)	**0.008**
Associated Findings										
Cavity	0		6	(12.5)	0.055	4	(57.1)	2	(2.9)	**< 0.001**
Mediastinal lymphadenopathy	3	(11.1)	5	(10.4)	0.925	1	(14.3)	7	(10.3)	0.745
Hilar lymphadenopathy	5	(18.5)	7	(14.6)	0.655	0		12	(17.6)	0.225
Pleural effusion	2	(7.4)	6	(12.5)	0.493	1	(14.3)	7	(10.3)	0.745
Location and Distribution										
Unilateral (Right)	11	(40.7)	17	(35.4)	0.647	2	(28.6)	26	(38.2)	0.615
Unilateral (Left)	16	(59.3)	15	(31.3)	**0.018**	2	(28.6)	29	(42.6)	0.471
Bilateral	0		16	(33.3)	**< 0.001**	3	(42.9)	13	(19.1)	0.144
Focal	26	(96.3)	24	(50.0)	**< 0.001**	3	(42.9)	47	(69.1)	0.161
Multifocal	1	(3.7)	19	(39.6)	**< 0.001**	3	(42.9)	17	(25.0)	0.309
Diffuse	0		5	(10.4)	0.083	1	(14.3)	4	(5.9)	0.396

bias. Another limitation is that clinical and laboratorial data weren't available. A larger sample would have resulted in a greater generalizability of our imaging findings. Consequently, further multicentric studies, particularly prospective cohorts, would be necessary to overcome these limitations and provide a better generalization of our results.

5. Conclusions

In our study population, the main etiologies found in patients with granulomatous disease who underwent lung biopsy were fungal or mycobacterial disease, specially histoplasmosis and tuberculosis, and nodular pattern with focal distribution was the most common imaging finding, detected with substantial interreader agreement.

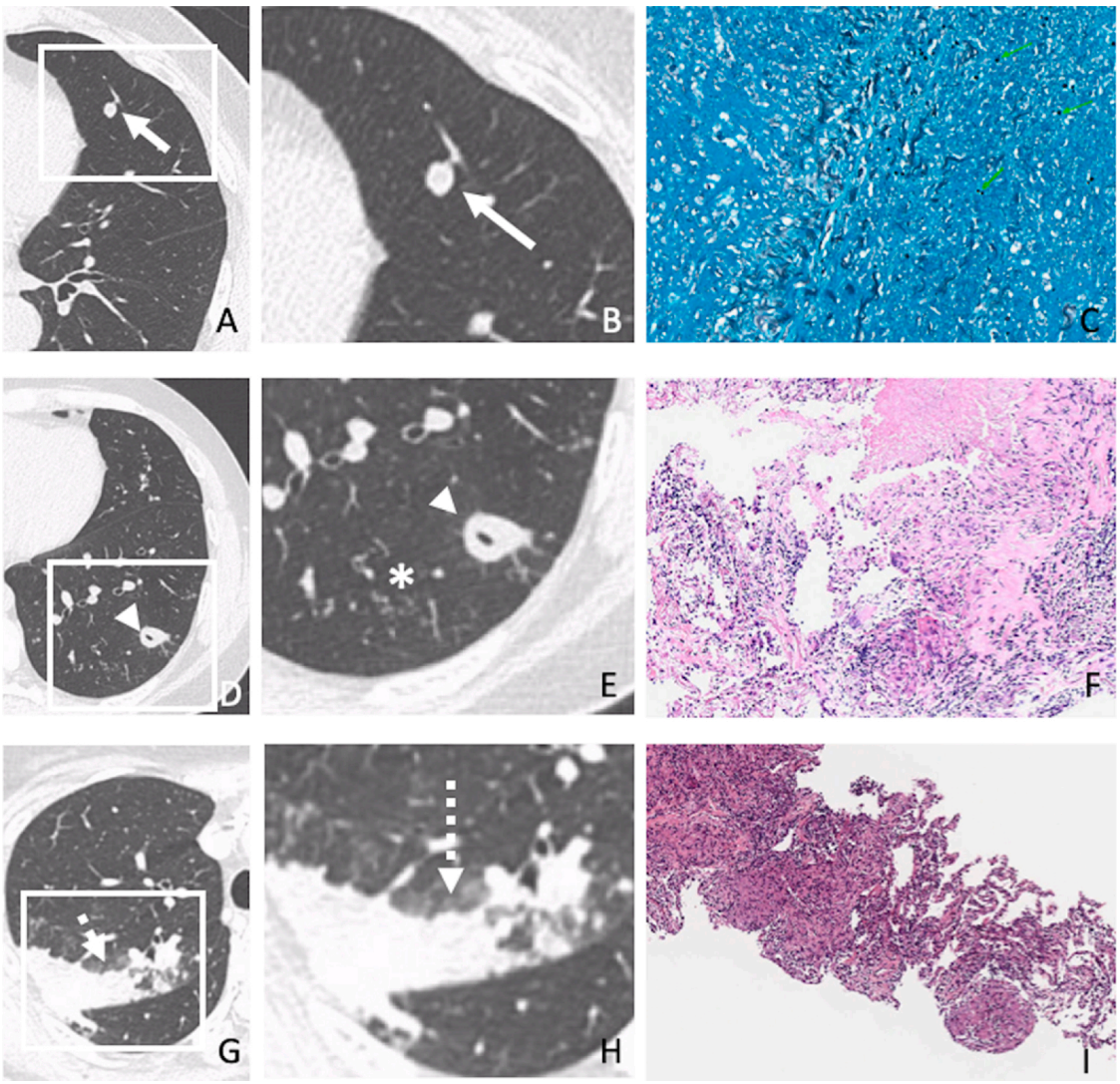

Fig. 5. Radiologic-pathologic correlation of three sample cases of our population. (A-C) 52-year-old patient with histoplasmosis. Chest CT (A) and enlarged image (B) demonstrating a solitary pulmonary nodule (arrows). (C) Lung biopsy showed necrotizing granulomatous inflammation with Histoplasma capsulatum yeasts (GMS 400x). (D-F) 34-year-old patient with tuberculosis. Chest CT (D) and enlarged image (E) demonstrating cavitated nodule (arrowheads) and centrilobular micronodules (asterisk). (F) Lung biopsy showed necrotizing granulomatous inflammation (HE 50x) consistent with tuberculosis. (G-I) 54-year-old patient with sarcoidosis. Chest CT (G) and enlarged image (H) showing consolidation (dashed arrows). (I) Lung biopsy depicted non-necrotizing granulomatous inflammation (HE 50x) consistent with sarcoidosis.

Funding

No funding.

Ethics approval and consent to participate

The institutional ("Comitê de Ética em Pesquisa do Hospital Sírio-Libanês" – Research Ethics Committee of the Hospital Sírio-Libanês) and national ("Comissão Nacional de Ética em Pesquisa do Conselho Nacional de Saúde CEP/CONEP" - National Research Ethics Commission of the National Health Council) review boards approved our retrospective study.

Research Ethics Committee of the Hospital Sírio-Libanês Registration Number 844

CEP/CONEP's Registration Number 03433918.9.0000.5461.

Consent for publication

The institutional and national review boards approved our retrospective study and waived the requirement for informed consent.

Declaration of Competing Interest

The authors declare that they have no known competing financial interests or personal relationships that could have appeared to influence the work reported in this paper.

CRediT authorship contribution statement

Camila Vilela de Oliveira: Study concepts; literature search; patient selection; interpretation of data; manuscript drafting and edition; approval of final version of submitted manuscript.

Natally Horvat: Study concepts; study design; interpretation of data; manuscript drafting and edition; approval of final version of submitted manuscript.

Leonardo de Abreu Testagrossa: Performed the histological review; approval of final version of submitted manuscript.

Davi dos Santos Romão and Marina Bastos Rassi: Junior radiologists

who performed the image review; approval of final version of submitted manuscript.

Hye Ju Lee: Conception; senior radiologist who performed the image review; review of the manuscript; approval of final version of submitted manuscript.

Appendix A. Supplementary data

Supplementary material related to this article can be found, in the online version, at doi:https://doi.org/10.1016/j.ejro.2021.100325.

References

[1] Q. Zhu, X. Xu, M. Li, X. Wang, Analysis of chest computed tomography manifestations of non-Mycobacterium tuberculosis induced granulomatous lung diseases, Radiology of Infectious Diseases (2017) 157–163.

[2] X. Yang, J. He, J. Wang, W. Li, C. Liu, D. Gao, et al., CT-based radiomics signature for differentiating solitary granulomatous nodules from solid lung adenocarcinoma, Lung Cancer 125 (2018) 109–114.

[3] S. Ohshimo, J. Guzman, U. Costabel, F. Bonella, Differential diagnosis of granulomatous lung disease: clues and pitfalls: Number 4 in the Series "Pathology for the clinician" Edited by Peter Dorfmüller and Alberto Cavazza, Eur Respir Rev. 26 (145) (2017).

[4] A.C. Nachiappan, K. Rahbar, X. Shi, E.S. Guy, E.J. Mortani Barbosa, G.S. Shroff, et al., Pulmonary Tuberculosis: Role of Radiology in Diagnosis and Management, Radiographics. 37 (1) (2017) 52–72.

[5] WHO, Global tuberculosis report 2019, World Health Organization, Geneva, 2019.

[6] R. Aljadani, A.E. Ahmed, H. Al-Jahdali, Tuberculosis mortality and associated factors at King Abdulaziz Medical City Hospital, BMC Infect Dis. 19 (1) (2019) 427.

[7] S. Mukhopadhyay, A.A. Gal, Granulomatous lung disease: an approach to the differential diagnosis, Arch Pathol Lab Med. 134 (5) (2010) 667–690.

[8] O.A. El-Zammar, A.L. Katzenstein, Pathological diagnosis of granulomatous lung disease: a review, Histopathology. 50 (3) (2007) 289–310.

[9] R.S. Dagaonkar, C.V. Choong, A.B. Asmat, D.B. Ahmed, A. Chopra, A.Y. Lim, et al., Significance of coexistent granulomatous inflammation and lung cancer, J Clin Pathol. 70 (4) (2017) 337–341.

[10] C. Danese, M. Cirene, M. Colotto, A singular case of granulomatous lesions of unknown significance, Minerva Med. 99 (2) (2008) 213–218.

[11] D.M. Hansell, A.A. Bankier, H. MacMahon, T.C. McLoud, N.L. Müller, Remy J. Fleischner Society, glossary of terms for thoracic imaging, Radiology. 246 (3) (2008) 697–722.

[12] J.R. Landis, G.G. Koch, The measurement of observer agreement for categorical data, Biometrics 33 (1) (1977) 159–174.

[13] S. Mukhopadhyay, C.F. Farver, L.T. Vaszar, O.J. Dempsey, H.H. Popper, H. Mani, et al., Causes of pulmonary granulomas: a retrospective study of 500 cases from seven countries, J Clin Pathol. 65 (1) (2012) 51–57.

[14] A. Nazarullah, R. Nilson, D.J. Maselli, J. Jagirdar, Incidence and aetiologies of pulmonary granulomatous inflammation: a decade of experience, Respirology. 20 (1) (2015) 115–121.

[15] Y. Sakakibara, Y. Suzuki, T. Fujie, T. Akashi, T. Iida, Y. Miyazaki, et al., Radiopathological Features and Identification of Mycobacterial Infections in Granulomatous Nodules Resected from the Lung, Respiration. 93 (4) (2017) 264–270.

[16] F.F. Gazzoni, L.C. Severo, E. Marchiori, K.L. Irion, M.D. Guimarães, M.C. Godoy, et al., Fungal diseases mimicking primary lung cancer: radiologic-pathologic correlation, Mycoses. 57 (4) (2014) 197–208.

[17] S. Chong, K.S. Lee, C.A. Yi, M.J. Chung, T.S. Kim, J. Han, Pulmonary fungal infection: imaging findings in immunocompetent and immunocompromised patients, Eur J Radiol. 59 (3) (2006) 371–383.